Cellulose (2018) 25:7315–7328
https://doi.org/10.1007/s10570-018-2077-8

ORIGINAL PAPER

Synthesis of lignocellulose-based composite hydrogel as a novel biosorbent for Cu^{2+} removal

Lili Zhang · Hailong Lu · Juan Yu · Yimin Fan · Yiqin Yang · Jinxia Ma · Zhiguo Wang

Received: 17 June 2018 / Accepted: 2 October 2018 / Published online: 6 October 2018

Abstract A lignocellulose-based composite hydrogel, as a novel biosorbent, was prepared for Cu^{2+} removal from wastewater. TEMPO-oxidized cellulose nanofibrils (TOCN) were dispersed in a 7 wt% NaOH/12 wt% urea aqueous solution at room temperature. Meanwhile, the dissolved cellulose was obtained in the same system at subzero temperature. The composite hydrogels were prepared by blending the dissolved cellulose solution, TOCN dispersion, and alkali lignin solution in an NaOH/urea aqueous solution. The composite hydrogel exhibits excellent adsorption capacity for heavy metals, which can be attributed to the synergistic effects of physical adsorption (porous 3D structure) and chemical adsorption (active sites: carboxyl and phenolic groups). The maximum amount of adsorbed Cu^{2+} onto composite hydrogel can reach 541 mg/g, which was achieved after 45 min. The adsorption behavior is well-described by the pseudo-second-order kinetics and the Freundlich model ($R^2 > 0.999$). Furthermore, the composite hydrogel exhibits high-strength properties, indicating that the presence of TOCN and lignin contributes to mechanical improvements.

Electronic supplementary material The online version of this article (https://doi.org/10.1007/s10570-018-2077-8) contains supplementary material, which is available to authorized users.

L. Zhang · H. Lu · J. Yu · Y. Fan · Y. Yang · J. Ma · Z. Wang
Jiangsu Co-Innovation Center of Efficient Processing and Utilization of Forest Resources, Nanjing Forestry University, Nanjing 210037, China

Z. Wang (✉)
College of Light Industry and Food Engineering, Nanjing Forestry University, Longpan Road 159, Nanjing, China
e-mail: wzg@njfu.edu.cn

Graphical abstract

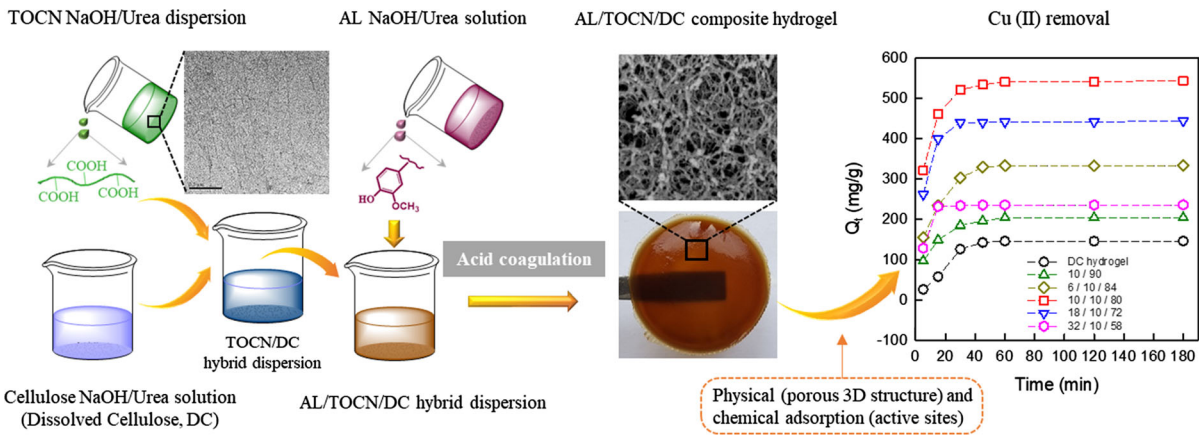

Keywords Biosorbent · Lignin · TOCN · Composite hydrogel · Copper ion removal

Introduction

Heavy metal contamination in water has become a serious environmental problem with the development of industry and causes significant threats to human health and the ecosystem due to these metals' toxicity (Xiong et al. 2014; Mahfoudhi and Boufi 2017; Ciesielczyk et al. 2017). Cu^{2+} is one of the most toxic metallic ions, which is produced by the copper smelter. Conventional methods for removing toxic heavy metal from wastewater include adsorption (Zhao et al. 2016; Suhas et al. 2016), membrane separation (Sotto et al. 2014), photocatalysis (Wang et al. 2016), ion exchange (Carro et al. 2015), and chemical precipitation (Xu et al. 2015). Among these methods, adsorption is preferred due to its good recyclability, easy operation, and the availability of various adsorbents (Duan et al. 2013). Recently, biomass adsorbents have received great attention because of their advantages of being low-cost and environmentally friendly with high efficiency, as shown in Table 1 (Gautam et al. 2014). However, the most of adsorbents based on biomass is not easy to separate from wastewater and possesses low adsorption capacity.

Bio-based hydrogels, possessing abundant functional groups and 3D porous structures, have been widely utilized for heavy metal removal (Zhu and Li 2015; Mohammadi et al. 2017). Hydrogel-based biosorbents are designed and synthesized from naturally abundant materials [e.g., chitosan (Ma et al. 2017), guar gum (Dai et al. 2017), cellulose (Isobe et al. 2013), and lignin (Li et al. 2015b)]. Cellulose, as the most abundant biopolymer in nature, is an excellent candidate for gel fabrication (Wang et al. 2012, 2017). Isobe et al. (2013) reported that cellulose hydrogel possessed favorable interactions with Cu^{2+} and has a high adsorption capacity after introducing carboxyl groups onto the surface via TEMPO oxidation. Ma et al. (2018) used waste cotton fabrics (WCFs) and polyacrylamide to fabricate a double network hydrogel for removing metal ion contamination, and further conforming the crosslinking density of the hydrogel network greatly affects its adsorption performance.

Usually, the high adsorption capacities of cellulose-based adsorbents are mainly achieved through introduction of functional groups on cellulose via oxidation, halogenation, esterification, and grafting methods (Sehaqui et al. 2014). However, these modification methods would inevitably pollute the environment to some extent due to the use of toxic chemicals. The adsorption capacity of a raw cellulose adsorbent without modification could not be as high as expected due to the lack of strong binding sites for metal ions (Kamel et al. 2006).

Lignin, as a byproduct of the paper and pulp industry, includes large amount of polar functional groups, such as benzyl alcohol, carbonyl, hydroxyl, and phenolic groups (Erdtman 1972; Pang et al. 2017). These groups are capable of binding heavy metal ions

Table 1 The adsorption capacity of different sorbents based on biomass for Cu^{2+} removal from waste water

Adsorbent based on biomass	Adsorption capacity (mg/g)	References
Cellulose-g-acrylic acid copolymer	330.9	Hajeeth et al. (2013)
Modified-Nanocellulose	201.6	Hokkanen et al. (2014)
TEMPO-mediated oxidized cellulose	52.3	Zhang et al. (2016)
Lignin/inorganic hybrid	84.0	Ciesielczyk et al. (2017)
Dithiocarbamate lignin	175.9	Ge et al. (2014)
Chitosan/rectorie nano-composite	20.5	Zeng et al. (2015)
Cotton fabrics hydrogel	138.9	Ma et al. (2018)

through chelation (Pagnanelli et al. 2003), which suggests that lignin has the ability to be used as a low-cost adsorbent for removing heavy metals from wastewater (Ahmaruzzaman 2011). Srivastava et al. (1994) utilized extracted lignin from black liquor to remove heavy metal contamination from an aqueous solution and obtained high adsorption capacity for Zn^{2+} and Pb^{2+}, reaching 73 and 1587 mg/g, respectively. Guo et al. (2008) utilized isolated lignin from black liquor to remove the heavy metal ions Ni^{2+}, Zn^{2+}, Cd^{2+}, Cu^{2+}, and Pb^{2+}. The results demonstrated that the carboxylic- and phenolic-type surface groups of lignin have strong attractions to metal ions. Li et al. (2015a) synthesized a porous lignin-based biosorbent for Pb^{2+} removal, which showed that the porous structure exposes a large amount of active sites, and benefits for the adsorption of lead ions. Thus, the loading of lignin on hydrogel-based adsorbents contributes to improving the adsorption capacity of the adsorbents. In addition, the porous structure of the hydrogel improves the dispersibility of lignin, exposing many active sites for complexing and coordination of metal ions.

The mechanical strength of adsorbents is important for practical applications. TEMPO-oxidized cellulose nanofibrils (TOCN), due to their "green" features (biocompatibility, biodegradability, renewability) and high crystallinity, are considered ideal candidates for use as reinforcing fillers in polymer nanocomposites (Liu et al. 2018; Safwat et al. 2018). Qi et al. (2009) prepared an all-cellulose composite film based on native cellulose nanofibers as the reinforcing phase and dissolved cellulose as the matrix, providing a pathway for the preparation of biodegradable nanocomposites. Fujisawa et al. (2016) reported the preparation process of a cellulose nanofibrils/regenerated cellulose composite film, demonstrating that TOCN improves mechanical properties of resultant nanocomposites. In addition, TOCN has been reported to have C6 carboxyl groups, which can bind with heavy metals, thereby improving the adsorption capacity of the resultant biosorbent.

In this study, a high-efficiency and composite hydrogel was obtained as a biosorbent for Cu^{2+} removal (compared with the previous results as shown in Table 1). The TOCN were dispersed in 7 wt% NaOH/12 wt% urea aqueous solution at room temperature. Meanwhile, the dissolved cellulose was obtained in the same system at subzero temperature. The composite hydrogels were fabricated by blending the TOCN dispersion, cellulose solution, and alkali lignin (AL) in an NaOH/urea aqueous solution based on their temperature-dependent solubility. The properties of the obtained hydrogel were analyzed using N_2 adsorption–desorption measurements, Fourier transform infrared spectroscopy (FTIR), scanning electron microscopy (SEM), and rheological and compression tests. More importantly, the feasibility of the composite hydrogel for removing Cu^{2+} ions was determined.

Experimental

Materials

Cellulose samples were prepared from poplar wood chips by the kraft pulping process and later bleached with sodium hypochlorite in the laboratory (Zhang et al. 2017). The degree of polymerization (DP) of cellulose decreased to 367 through acid hydrolysis, as described in a previous study (Shi et al. 2015). TEMPO-oxidized cellulose nanofibrils (TOCN) were prepared by chemical oxidation and mechanical treatment of cellulose (Isogai et al. 2011). The degree of polymerization and carboxylate content of TOCN is 190 and 1.191, respectively. Alkali lignin (AL, M_W:

5100) was obtained from a paper mill in Jiangsu province, China. Prior to the experiments, the AL was purified by acid precipitation and centrifugation (Minu et al. 2012).

Sodium hydroxide (NaOH), urea, sodium hypochlorite (NaClO), TEMPO, sodium bromide (NaBr), and other chemicals were bought from Shanghai Aladdin Chemical Co. Ind., China. All reagents were of analytical grade and used without further purification.

Preparation of AL/TOCN/DC composite hydrogels

Dissolved cellulose, abbreviated as DC, was prepared with the NaOH/urea/H_2O solvent system (Cai and Zhang 2005). 7 g NaOH and 12 g urea were dissolved in 81 g H_2O to prepare alkali urea solvent system (7 wt% NaOH/12 wt% urea aqueous solution), according to the previous reported method (Cai and Zhang 2005; Shi et al. 2018). A cellulose with DP 367 was dispersed in 7 wt% NaOH/12 wt% urea aqueous solution. After being frozen and thawed, the mixture was vigorously stirred for 5 min to give a transparent cellulose solution with 3 wt% solid content as the dissolved cellulose sample (DC).

Various concentrations of TOCN NaOH/urea aqueous dispersions were prepared by adding drops to the desired amount of 7 wt% NaOH/12 wt% aqueous solution to a TOCN aqueous dispersion. Next, TOCN NaOH/urea aqueous dispersions were stirred for 30 min at room temperature. Meanwhile, the desired amount of AL (M_W: 5100) was added to the 7 wt% NaOH/12 wt% urea aqueous solution to obtain various concentrations of AL NaOH/urea aqueous solutions followed by stirring to produce a clear AL solution.

The preparation process of the AL/TOCN/DC composite gels is shown in Fig. 1. After the dissolved cellulose NaOH/urea aqueous solution warmed up to room temperature, the TOCN NaOH/urea aqueous dispersion was added dropwise, and the AL NaOH/urea aqueous solution was also added. The mixture was stirred for 30 min. In order to study effect of TOCN on the properties of composite hydrogel, the ratios of TOCN/DC were designed from 0/100 to 15/85 since TOCN were used as reinforcing fillers in component hydrogel. Moreover, in order to study the effect of AL, the ratios of AL/TOCN/DC were designed from 6/10/84 to 32/10/58. The ratios of three components were based on oven dry mass of materials. The concentration of mixture solution is 1.84 wt% (oven dry). The resulting TOCN/DC mixtures and AL/TOCN/DC mixtures were poured into the glass dish to mold. Hydrochloric acid (HCl, 1 M) was added to the coagulation bath as a gelling agent. After gelation, the hydrogels were soaked in distilled water to exchange solvents. Finally, the available biosorbent can be obtained when the pH of the rinsing water approaches neutral.

Characterization

Rheology measurements

Rheological tests of composite hydrogels were conducted using an RS6000 Rheometer (HAAKER, German). A P20 TiL Platte and a P20 TiL cone plate can be used. The specimens were subjected to a strain-sweep test over the range of 1–10^4 Pa at ambient temperature. Storage modulus (G') and loss modulus (G'') were recorded for lignocellulose gels. The samples were measured three times.

Structure analysis

Various LC aerogels were produced from LC hydrogels via freeze-drying for 3 days. The morphology and pore structure of aerogels were imaged on a JEOL-JSM 7600F scanning electron microscope (SEM) (Tokyo, Japan). Before examination, the LC aerogels were coated with gold. EDX analysis was conducted using an energy dispersive X-ray spectrometer that was installed on an SEM (JEOL 7600F).

BET analysis was conducted using a V-Sorb 2800P (Gold APP, China) analyzer with N_2 gas as the adsorbate. Moisture was removed from the samples by degassing at 100 °C for 8 h before examination.

FT-IR spectra of composite hydrogels were obtained on a VERTEX 80 V spectrometer (Bruker, Germany) in the region of 4000–400 cm^{-1}. X-ray diffraction (XRD) of composite hydrogels was performed on a multi-function X-ray diffractometer (Ultima-IV). The diffraction angle 2θ was from 4° to 50° under 40 kV and 30 mA.

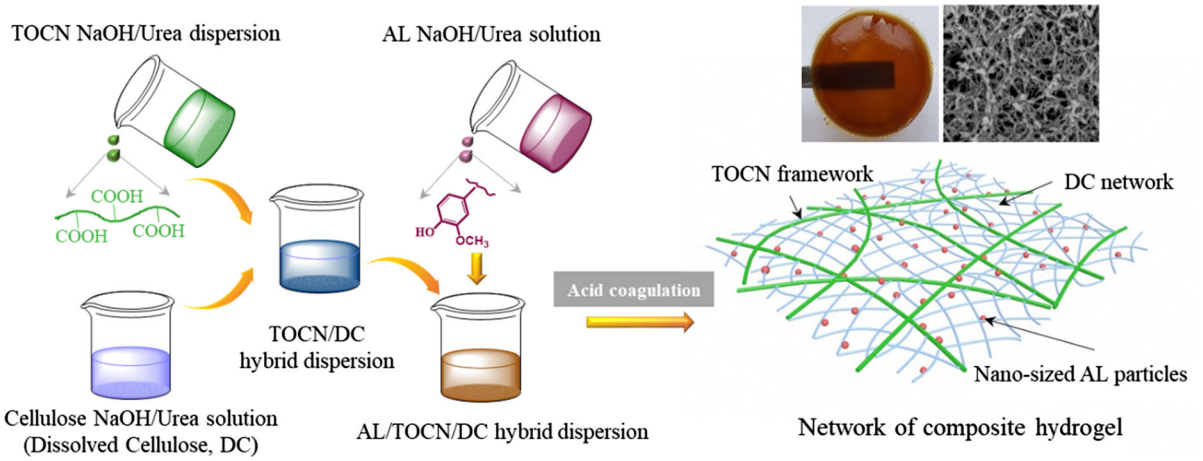

Fig. 1 Preparation of AL/TOCN/DC composite hydrogels

Cu^{2+} adsorption on composite hydrogels

The effects of contact time (0–300 min) and adsorption isotherms (initial concentration 50–250 mg/L) of Cu^{2+} on the adsorption of composite hydrogels were investigated. Various $CuSO_4$ solutions with concentrations varying from 50 to 250 mg/L were obtained by dissolving $CuSO_4$ in deionized water. The composite hydrogels (45 mg, oven dried) were placed into a conical flask with 100 mL $CuSO_4$ aqueous solution. The mixtures were shaken for 24 h using a thermostatic shaker (MaxQ4000, Thermo Scientific, America) at 25°C and 100 rpm. Cu^{2+} concentration was measured using the SK-2002 B atomic absorption spectrophotometer (Beijing, China). Equation (1) was used to determine the amounts of Cu^{2+} adsorbed on the hydrogel:

$$Q_e = \frac{V(C_0 - C_e)}{m} \quad (1)$$

where C_0 and C_e are the initial and equilibrium concentrations of Cu^{2+} (mg/L), respectively, V is the volume of $CuSO_4$ solution (L) and m is the oven dry mass of the prepared hydrogel (g).

Results and discussion

Preparation of AL/TOCN/DC composite hydrogels

The main objective of this work is to fabricate high-strength, porous composite hydrogels with excellent adsorption properties for metal ions. The concept in the design of the hydrogel is that the composition of DC, TOCN, and AL through a co-blending method can retain the properties of these materials. The final hydrogel-based adsorbent is formed based on the interpenetrating network of TOCN and DC, and the loading of lignin nanoparticles.

In the gelation process, TOCN can become the framework due to their high aspect ratio. A uniform distribution of TOCN is necessary to keep nanofibers from flocking together. Figure 2 shows the XRD spectra of freeze-dried TOCN before and after treatment with NaOH/Urea aqueous solution. The characteristic peaks of cellulose I in TOCN were almost unchanged after dispersing in NaOH/Urea aqueous solution, suggesting that NaOH/Urea aqueous solution is unable to dissolve TOCN at room temperature (Qi et al. 2009). Qi et al. (2009) prepared an all-cellulose composite film based on native cellulose nanofibers as the reinforcing phase and dissolved cellulose from NaOH-urea aqueous solution as the matrix. The cellulose nanowhiskers retained their needlelike morphology with mean length and diameter of 300 and 21 nm as well as native crystallinity when added to the latter solution at ambient temperature. Fujisawa et al. (2016) reported the preparation process of a cellulose nanofibrils/regenerated cellulose composite film, demonstrating the cellulose I crystal structure of nanofibrils is preserved after the treatment. The image of TOCN dispersion in NaOH/Urea observed between cross-polarizers shows clear birefringence (the inset of Fig. 2a).

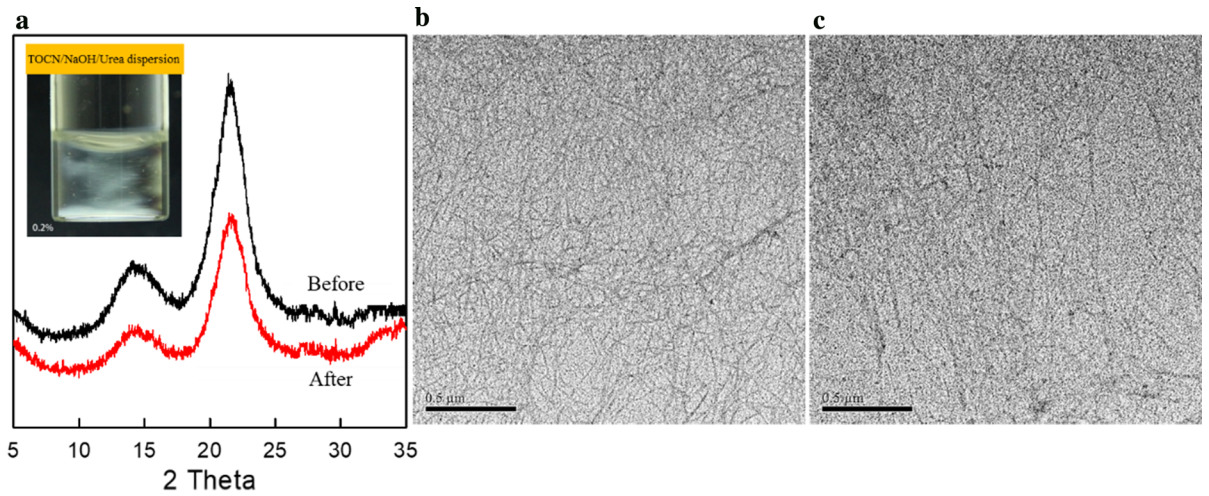

Fig. 2 XRD of freeze-dried TOCN before and after treatment with NaOH/Urea aqueous solution (**a**), image of TOCN dispersion in NaOH/Urea observed between cross-polarizers (the inset of **a**), and TEM of TOCN before (**b**) and after (**c**) treatment with NaOH/Urea aqueous solution

To study the morphological changes of TOCN in the NaOH/Urea aqueous solvent system at room temperature, TEM images of TOCN before and after treatment with NaOH/Urea aqueous solution were obtained and are shown in Fig. 2b, c. TOCN dispersed in water have TEMPO-oxidized nanofibers with a large aspect ratio (Fig. 2b) (Isogai et al. 2011). By being dispersed in NaOH/Urea aqueous solution and dialysis, the morphology of TOCN hardly changed (Fig. 2c). In other words, the solubility of cellulose in the NaOH/Urea aqueous solvent system depended on the reaction temperature.

Some studies suggest that lignin components tend to associate with one another in both aqueous and ethanol media (Lindströmn 1979; Gidh et al. 2006; Guerra et al. 2007). Xu et al. (2007) demonstrated the re-sorption and precipitation behavior of dissolved lignin in the ethanol pulping and washing process, and observed that a large amount of spherical lignin particles appeared. In this work, AL is dissolved in NaOH/Urea aqueous solution and regenerated with hydrochloric acid. During regenerating process, dissolved lignin is readily to form lignin nanoparticles (LNPs) to be adsorbed and deposited on regenerated cellulose network due to its hydrophobic association. As shown in Fig. 1, during the gelation process, hydrochloric acid is used as a coagulating agent for gel formation and a neutralizing agent for alkaline solvents. The presence of hydrochloric acid provides an acidic environment, contributing to precipitation and retention of alkaline lignin in the gel structure.

Through the co-blending method, TOCN can effectively introduce carboxyl groups, contributing to the adsorption of metal ions on the composite hydrogel. TOCN also reinforce the mechanical strength of the gel, due to having a higher aspect ratio (Xu et al. 2013). Furthermore, lignin contains two main types of active sites (phenolic- and carboxylic-groups) (Guo et al. 2008), which have a high affinity for metal ions, and thus improve the adsorption capacities of resultant hydrogels. The formation of nanosized lignin particles can further strengthen the mechanical properties of composite hydrogels. The lignin nanoparticles can be used as fillers in the gel network. In addition, the interpenetrating web-structure of hydrogels is based on the framework of TOCN, the filling network of dissolved cellulose, and the loading of lignin nanoparticles. The composite hydrogel has a large specific area and a rich pore structure, which accounts for its excellent adsorption properties. Therefore, we believe the AL/TOCN/DC composite hydrogels not only have excellent performance but can also be applied to the efficient removal of heavy metals from wastewater.

Properties of composite hydrogels

The mechanical strength of adsorbents is important for practical application. The viscoelastic properties of

composite hydrogels are shown in Fig. 3. The storage modulus G' represents stored energy in materials during elastic deformation, which reflects the elasticity property of materials; the loss modulus G'' represents the lost energy due to viscous deformation, which reflects viscosity property (Mushi et al. 2016). In other words, storage modulus G' exhibits the stiffness of materials (Liu et al. 2016). Moreover, the cross point of G′ and G″ is the critical value indicating that the hydrogel can bear the shear stress before irreversible deformation. As shown in Fig. 3, G' values are much higher than G'' for all hydrogels over the whole stress range, implying elastic gel characteristics.

Figure 3a presents the effect of TOCN addition on the viscoelastic properties of TOCN/DC composite hydrogels. It can be observed that the composite hydrogels containing TOCN have much higher strength than the DC hydrogel, confirming that TOCN are responsible for the excellent mechanical properties of hydrogels. The TOCN/DC (10/90) composite hydrogel shows a higher storage modulus and loss modulus than others. The strengths of hydrogels decrease slightly when the addition of TOCN is up to 15 wt% (o.d.), which is attributed to flocculation occurring for a high concentration of nanofibers.

The effect of AL addition on the viscoelastic properties of AL/TOCN/DC composite hydrogels is shown in Fig. 3b. The presence of AL can lead to mechanical enhancement of the composite hydrogels, which is due to the formation of AL nanoparticles as rigid fillers in the hydrogel network. The formation of nanosized AL particles is attributed to the hydrophobic association of AL molecules with each other in water or ethanol (Guerra et al. 2007). When the addition of AL exceeds 10 wt%, the strength of the composite hydrogel decreases slightly, since the presence of many lignin particles would weaken the interactions between cellulose chains during the formation of the composite hydrogel. Thus, the additions of 10 wt% AL and 10 wt% TOCN can maximize the improvement of the mechanical properties of the composite hydrogel, in which G' and G'' can reach up to 131 kPa and 13 kPa, respectively. The AL/TOCN/DC (10/10/80) composite hydrogel is also able to sustain a highest stress value of 20 kPa.

To observe the pore structure and micromorphology of composite hydrogels, freeze-dried composite aerogels were characterized using SEM and BET analysis. Cross-sectional SEM images of composite gels are shown in Fig. 4. All the gels show a three-dimensional highly porous network structure formed by randomly oriented fibrils. Compared to pure DC gel (porosity: 94.3%, S_{BET}: 109.6 m^2 g^{-1}), the TOCN/DC (10/90) composite gel exhibits a more abundant pore structure (porosity: 96.5%) and higher specific surface area (S_{BET}: 128.2 m^2 g^{-1}), indicating that the presence of TOCN improves the interconnection and entanglement of cellulose chains. In fact, it is difficult to distinguish the TOCN from DC fibrils. The TOCN/DC complex exhibits good miscibility due to abundant hydroxyl groups forming hydrogen bonds. Thus, a high level of intermixing and interpenetration network formed between TOCN and DC fibrils can result in improvement of pore structure and mechanical enhancement of composite hydrogels.

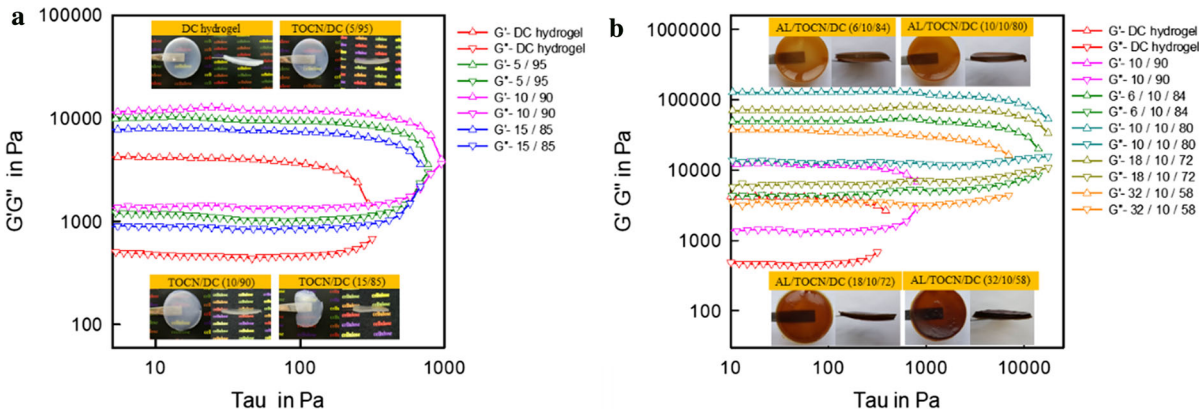

Fig. 3 Viscoelasticity of composite hydrogels with different mass ratios (o. d.) of TOCN/DC from 0/100 to 15/85 (**a**); and different lignin contents, with mass ratio (o. d.) of AL/TOCN/DC from 6/10/84 to 32/10/58 (**b**)

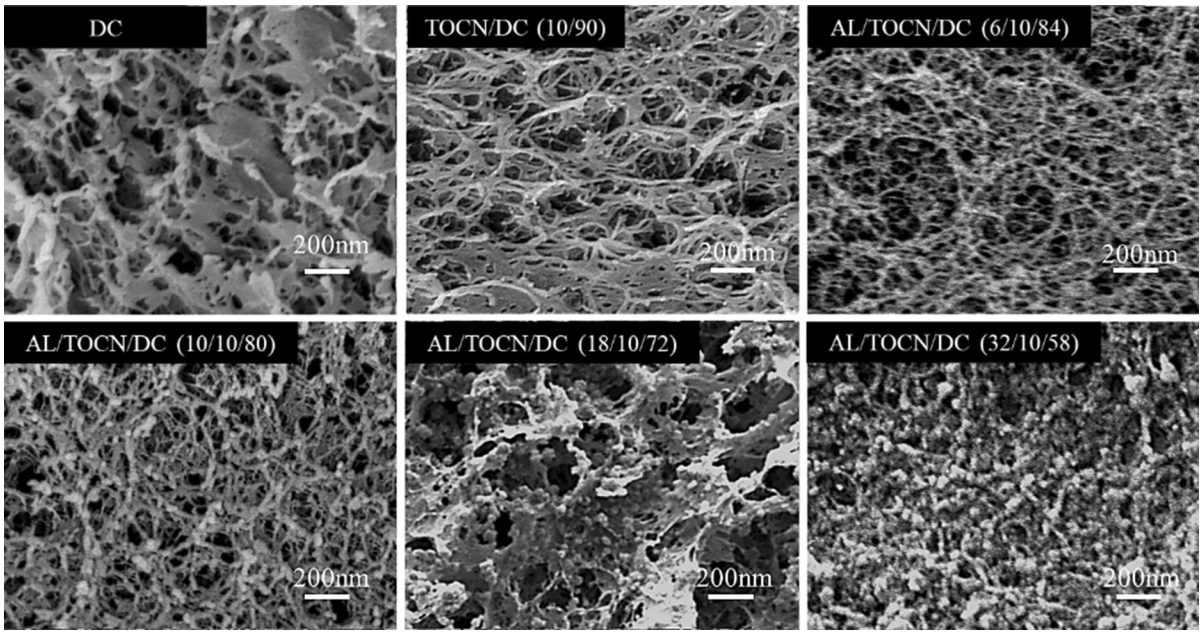

Fig. 4 SEM images of composite hydrogels

For the network of AL/TOCN/DC composite hydrogels, it can be observed that more lignin nanoparticles (LNPs) are loaded on cellulose fibrils with increasing lignin addition, which is attributed to the association of lignin molecules during the formation of the hydrogel network. The networks of AL/TOCN/DC (6/10/84) hydrogel and AL/TOCN/DC (10/10/80) hydrogel are more uniform and have a smaller pore size than lignin-free hydrogels, thereby implying a richer pore structure and higher surface area of the hydrogels. Meanwhile, the network of AL/TOCN/DC (18/10/72) hydrogel appears to primarily consist of macropores and LNP-loading fibril layers. The network of AL/TOCN/DC (32/10/58) hydrogel is almost formed by LNP-loading fibril layers. This can be attributed to superabundant padding LNPs affect the pore network structure of the hydrogels, which results in the decrease of the gels' porosity and specific surface area.

The corresponding specific surface area of composite hydrogels is shown in Fig. 5a. The results show that the BET surface area varied between 72.9 and 135.2 $m^2\ g^{-1}$, among which the AL/TOCN/DC (10/10/80) hydrogel shows the highest value of 135.2 $m^2\ g^{-1}$, while the AL/TOCN/DC (32/10/58) hydrogel shows the lowest value of 72.9 $m^2\ g^{-1}$. Moreover, the porosities of hydrogels varied between 93.98% and 97.28%, among which the AL/TOCN/DC (10/10/80) hydrogel shows the highest value of 97.28%, while the AL/TOCN/DC (32/10/58) hydrogel shows the lowest value of 90.86%. The difference of porosity and specific surface is attributed to the effect of lignin, high-content lignin can form more lignin particle than low-content lignin filling in the hydrogel network, resulting in the heterogeneous network nanostructure. The result is in accordance with SEM results; therefore, the hydrogel surface area is influenced by its pore structure.

The functional group of the hydrogel is an important factor for adsorption efficiency. The carboxylate contents of composite hydrogels are shown in Fig. 5a. When TOCN are introduced, the carboxylate content significantly increases, which means that abundant carboxylate groups exist on TOCN surfaces. Furthermore, the carboxylate content increases gradually with increasing lignin content, implying that the presence of AL also provides carboxylate groups for the hydrogel. That is, the functional groups on lignin contain a certain amount of carboxylic groups.

Figure 5b presents the FTIR spectrum of the AL/TOCN/DC (10/10/80) composite hydrogel. The characteristic band at 3400 cm^{-1} and the peak at 2933 cm^{-1} originate from aromatic and aliphatic O–H, and methyl C–H stretching vibrations of cellulose

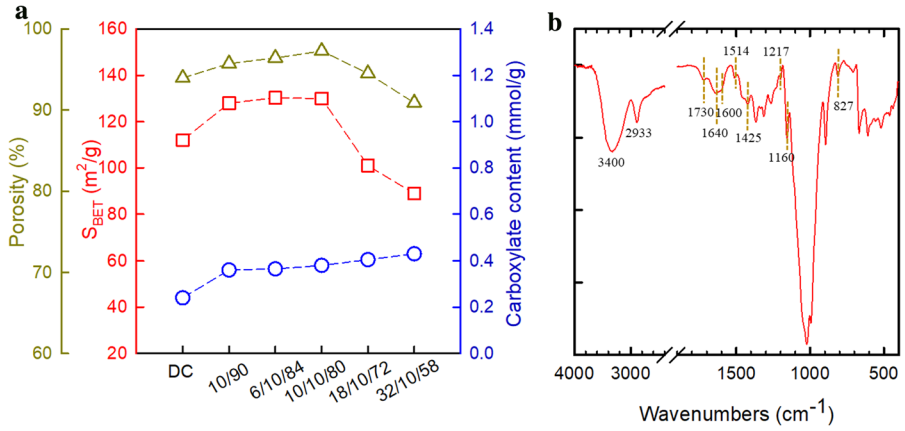

Fig. 5 Porosity, specific surface area and carboxylate content of composite hydrogels (**a**); FTIR of AL/TOCN/DC (10/10/80) composite hydrogel (**b**)

and lignin, respectively. The conventional bands for cellulose are noticed at 1640 and 1160 cm^{-1}, assigned to stretching vibrations of the O–H and C–O–C bonds, respectively (Qian and Sheng 2017). Three peaks at 1600, 1514 and 1425 cm^{-1} are dominated by the aromatic ring vibrations of lignin (Zhang et al. 2015).

Notably, the strong peak at 1730 cm^{-1} is attributed to carbonyl and conjugated carboxyl stretching, indicating the introduction of TOCN and lignin to the composite hydrogels. The peaks at 1217 and 827 cm^{-1} depict stretching vibrations of the syringyl ring. Thus, the signal is observed at 1217 and 1514 cm^{-1}, indicating that abundant phenolic groups exist on the lignin (Jung et al. 2015).

Removal of Cu^{2+} ions

The feasibility of using as-prepared AL/TOCN/DC composite hydrogel as a biosorbent for removing Cu^{2+} is assessed by analyzing its adsorption capacity. Figure 6a presents the effect of contact time on the adsorbed Cu^{2+} amount for various composite hydrogels. The adsorption behavior of composite hydrogels for Cu^{2+} can be divided into two stages. First, Cu^{2+} ions are diffused onto the surface of composite hydrogels from the solution; second, the Cu^{2+} ions further combine with active adsorption sites on the composite hydrogels by metal complexation. As shown, the adsorption capacity of AL/TOCN/DC (10/10/80) composite hydrogel for Cu^{2+} is the highest (541 mg/g), and that of DC hydrogel is the lowest (145 mg/g). The high Cu^{2+} adsorption capacity of the AL/TOCN/DC (10/10/80) composite hydrogel is attributed to two factors: (1) the composite hydrogel contains two major types of functional groups (phenolic and carboxylic groups from TOCN and lignin) that are able to produce complexation with metal ions (Guo et al. 2008; Zhang et al. 2016); (2) the composite hydrogel possesses a good porous 3D network, which provides the highest surface area and an abundant pore structure, leading to many active sites being exposed for the complexation of Cu^{2+} ions (Isobe et al. 2013; Zhu and Li 2015).

To reveal the relation between adsorption behavior and rate-controlling steps, two models [Lagergren pseudo first-order (Simonin 2016) and pseudo-second-order (Ho 2006)] are applied to analyze the adsorption kinetics of Cu^{2+} on the composite hydrogels. The linear pseudo first-order and pseudo-second-order were determined in accordance with Eqs. (2) and (3):

$$\log(Q_e - Q_t) = \log Q_e - \frac{k_1 t}{2.303} \quad (2)$$

$$\frac{t}{Q_t} = \frac{1}{k_2 Q_e^2} + \frac{t}{Q_e} \quad (3)$$

where Q_e and Q_t are the adsorption capacities of Cu^{2+} (mg g^{-1}) at equilibrium time and time t, respectively, and K_1 (min^{-1}) and K_2 (g/(mg min)) are the adsorption rate constants of the pseudo-first-order and pseudo second-order adsorption rates, respectively.

Figure 6b, c depicts the plots of lg ($Q_e - Q_t$) and (t/Q_t) versus t for the pseudo-first order and the pseudo-second-order models, respectively. The kinetic parameters can be calculated from the plots in Table 2. The

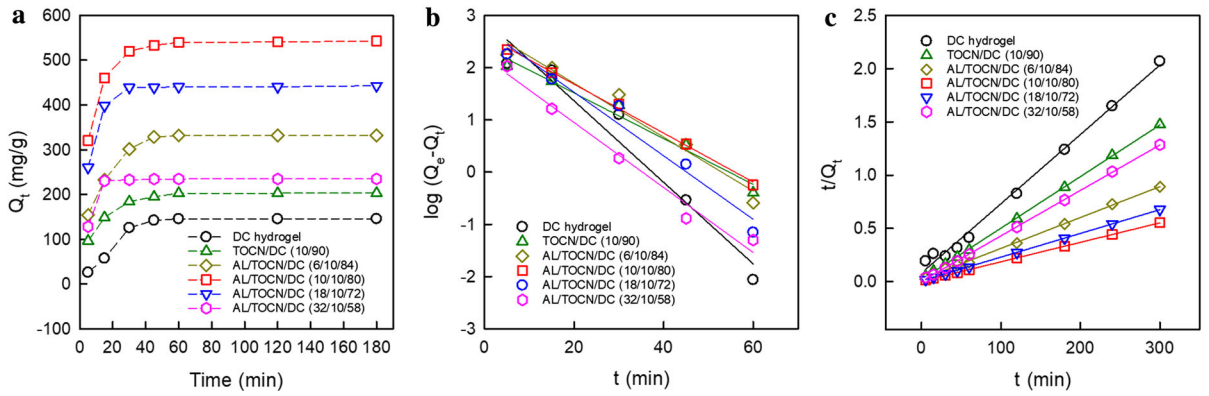

Fig. 6 Adsorption kinetics of Cu^{2+} onto the composite hydrogels (**a**), and the corresponding kinetic plots of pseudo-first-order (**b**) and pseudo-second-order (**c**) models for the adsorption of Cu^{2+}

correlation coefficients (R^2) of the pseudo-first-order model (0.952–0.987 for the composite hydrogels) are significantly lower than those of the pseudo-second-order adsorption model (0.994–0.999 for composite hydrogels). The theoretical Q_e values of the pseudo-second-order adsorption model are closer to the experimental results than those of the pseudo-first-order model. This finding suggests that the adsorption kinetics behaviors of hydrogels are well-fitted by the pseudo-second order model and that the adsorption behaviors between composite hydrogels and Cu^{2+} ions are dominated by chemical sorption via electron transfer (Mohan et al. 2006).

The diffusion and adsorption mechanism of Cu^{2+} ions into composite hydrogel is also clarified by the Weber and Morris intra-particle diffusion model (Eq. 4).

$$Q_t = k_{id} t^{\frac{1}{2}} + C \quad (4)$$

where Q_t (mg g^{-1}) is defined as adsorbed Cu^{2+} at time t; k_{id} is the rate constant of intra-particle diffusion, and C is a constant that is related to the thickness of the boundary layer (mg g^{-1}).

The plots of Q_t versus $t^{1/2}$ for the adsorption of Cu^{2+} into composite hydrogels are presented in Fig. 7, which shows nonlinear adsorption behavior. The intra-particle diffusion plots do not pass through the origin, indicating the existence of two or more adsorption mechanisms (Weber and Morris 1963). As shown, the adsorption process plots of Cu^{2+} into composite hydrogels include two stages: the fast stage and the equilibrium stage. Cu^{2+} ions move to the surface of various composite hydrogels from the solution, and then, Cu^{2+} moves into the interior parts to occupy available adsorption sites (Kumar et al. 2011). The AL/TOCN/DC (10/10/80) hydrogel gives the highest adsorption capacity, which is attributed to the largest surface area and richest adsorption sites. Therefore,

Table 2 Kinetic parameters of the pseudo-first-order and pseudo-second-order kinetic models for Cu^{2+} adsorption of the composite hydrogels

Adsorbent	$Q_{e,exp}$ (mg/g)	Pseudo-first-order kinetics			Pseudo-second-order kinetics		
		R^2	$Q_{e,cal}$	K_1 (min^{-1})	R^2	$Q_{e,cal}$	K_2 (g/mg min)
DC	145.56	0.952	833.87	0.179	0.994	153.84	0.0005
TOCN/DC (10/90)	203.14	0.974	243.84	0.101	0.999	208.33	0.0012
AL/TOCN/DC (6/10/84)	334.72	0.963	538.64	0.119	0.999	344.82	0.0004
AL/TOCN/DC (10/10/80)	540.72	0.987	413.90	0.108	0.999	555.556	0.0009
AL/TOCN/DC (18/10/72)	440.55	0.969	553.22	0.140	0.999	454.54	0.0006
AL/TOCN/DC (32/10/58)	234.81	0.979	155.34	0.143	0.999	232.56	0.0056

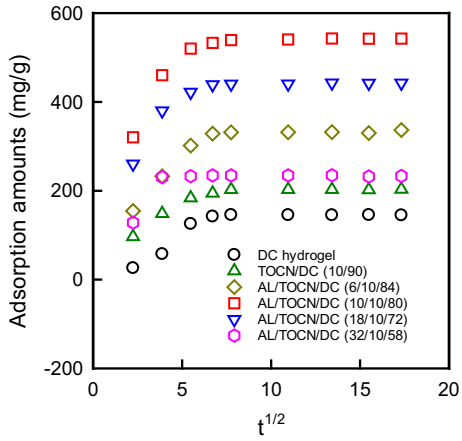

Fig. 7 Weber and Morris intra-particle diffusion plots of adsorption kinetics of the composite hydrogels

the adsorption of composite hydrogels for Cu^{2+} is dominated by multiple diffusion mechanisms.

The adsorption isothermal properties of the 10/10/80 (AL/TOCN/DC) composite hydrogel are investigated through determining the equilibrium adsorption capacity under varying initial Cu^{2+} concentrations, as shown in Fig. 8a. The adsorbed Cu^{2+} amount of the hydrogel evidently increases with initial Cu^{2+} concentration. The Langmuir (Eq. 5) and Freundlich isotherm models (Eq. 6) are used to analyze adsorption isotherm date.

$$\frac{C_e}{Q_e} = \frac{1}{Q_m k} + \frac{C_e}{Q_m} \tag{5}$$

$$\log Q_e = \log k_F + \frac{\log C_e}{n} \tag{6}$$

where Q_e (mg g^{-1}) and C_e (mg L^{-1}) are the Cu^{2+} concentration and equilibrium adsorption capacity, Q_m is the maximum adsorption capacity of hydrogel, and k (L mg^{-1}) is a constant of Langmuir isotherm models; k_F and n are constants of Freundlich isotherm models.

As indicated in Fig. 8b, c, Cu^{2+} adsorption onto the AL/TOCN/DC (10/10/80) composite hydrogel is

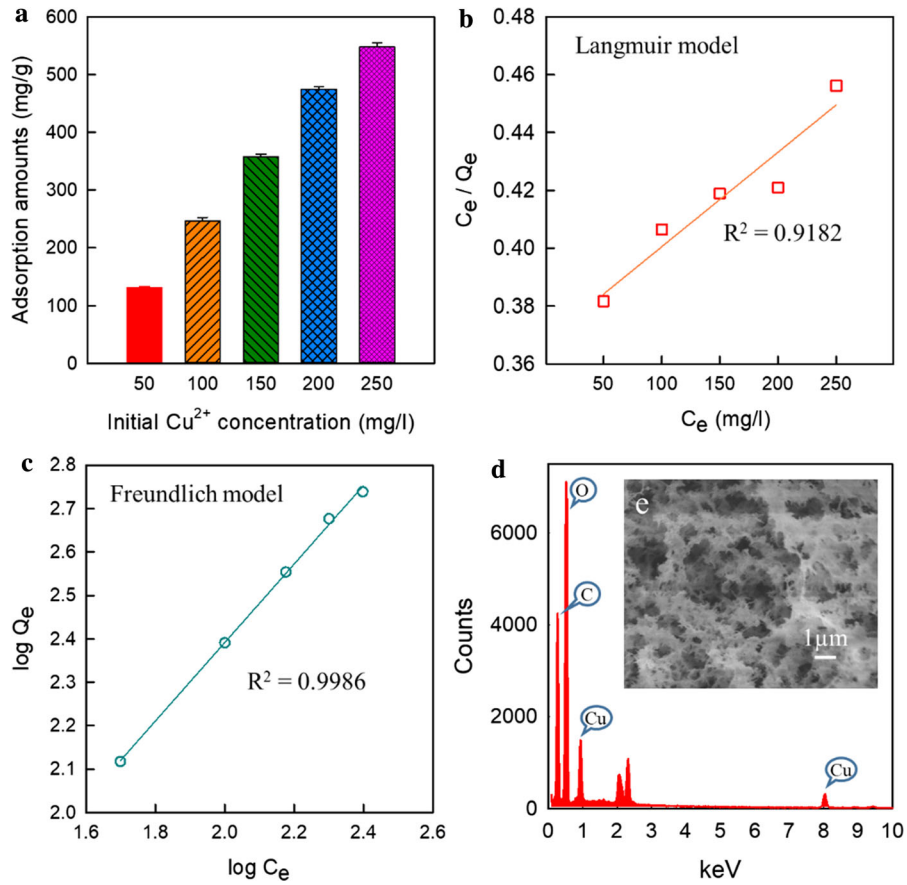

Fig. 8 Equilibrium adsorption amounts of Cu^{2+} on the AL/TOCN/DC (10/10/80) composite hydrogel at various starting Cu^{2+} concentrations (**a**); Cu^{2+} adsorption data fitted onto the Langmuir model (**b**); Cu^{2+} adsorption data fitted onto the Freundlich model (**c**); EDX analysis (**d**) and morphology structure (**e**) of the Cu^{2+}-adsorbed composite hydrogel

Table 3 Langmuir and Freundlich isothermal adsorption parameters of the composite hydrogels for Cu^{2+} removal

Adsorbent	$Q_{e,exp}$ (mg/g)	Langmuir model		Freundlich model	
AL/TOCN/DC (32/10/58)	540.72	R^2	0.9182	R^2	0.9986
		$Q_{e,cal}$ (mg/g)	563.33	n	2.48
		K_1 (mg/L)	0.1089	K_F	3.8326

better described by the Freundlich model (R^2 = 0.998) than the Langmuir model (R^2 = 0.918), which supports the multilayered adsorption mechanism of composite hydrogels. The Langmuir and Freundlich isothermal adsorption parameters of the composite hydrogels for Cu^{2+} removal was shown in Table 3.

The Cu^{2+}-adsorbed composite hydrogel is investigated using EDX analysis and SEM testing, as shown in Fig. 8d, e, respectively. After adsorption of Cu^{2+} ions, the copper element appears in the EDX spectrum of the composite, suggesting that Cu^{2+} ions are adsorbed successfully onto the composite hydrogel. That is, the composite hydrogels could be applied to heavy metal ion removal as a biosorbent.

Conclusion

A highly efficient hydrogel-based biosorbent with a porous structure was prepared for removing Cu^{2+} from wastewater. The composite hydrogels were fabricated by blending TOCN, AL, and cellulose solution in 7 wt% NaOH/12 wt% urea aqueous solution, which were based on the interpenetrating network of regenerated cellulose (as a matrix), TOCN (as a reinforcing agent) and lignin nanoparticles (as a filler). In this process, phenolic and carbonyl groups from lignin and TOCN are introduced into the hydrogel-based adsorbent, thereby improving the adsorption capacity of the resultant hydrogel. The porous structure of the hydrogel is also responsible for its excellent adsorption properties. The AL/TOCN/DC (10/10/80) composite hydrogel exhibits much higher adsorption capacity for Cu^{2+} (541 mg/g) than other composite hydrogels. The pseudo-second-order model is able to describe the adsorption kinetics of composite hydrogels accurately. The isotherm adsorption equilibrium data fit well to the Freundlich model. In addition, the composite hydrogel exhibits good mechanical property due to the presence of TOCN and lignin in the gel network. Thanks to the "green" gelation process, this novel biosorbent can be considered to be an eco-friendly and effective alternative for wastewater treatment in future industrial applications.

Acknowledgments We are grateful for financial support from National Key R&D Program of China (2017YFD0601005), as well as the National Natural Science Foundation of China (Grant No. 31870565), the Doctorate Fellowship Foundation of Nanjing Forestry University, the Postgraduate Research and Practice Innovation Program of Jiangsu Province (KYCX17_0845) and the Priority Academic Program Development of Jiangsu Higher Education Institutions (PAPD).

References

Ahmaruzzaman M (2011) Industrial wastes as low-cost potential adsorbents for the treatment of wastewater laden with heavy metals. Adv Colloid Interface Sci 166:36–59. https://doi.org/10.1016/j.cis.2011.04.005

Cai J, Zhang L (2005) Rapid dissolution of cellulose in LiOH/urea and NaOH/urea aqueous solutions. Macromol Biosci 5:539–548. https://doi.org/10.1002/mabi.200400222

Carro L, Barriada JL, Herrero R, Sastre de Vicente ME (2015) Interaction of heavy metals with Ca-pretreated Sargassum muticum algal biomass: characterization as a cation exchange process. Chem Eng J 264:181–187. https://doi.org/10.1016/j.cej.2014.11.079

Ciesielczyk F, Bartczak P, Klapiszewski Ł, Jesionowski T (2017) Treatment of model and galvanic waste solutions of copper(II) ions using a lignin/inorganic oxide hybrid as an effective sorbent. J Hazard Mater 328:150–159. https://doi.org/10.1016/j.jhazmat.2017.01.009

Dai L, Zhang L, Wang B et al (2017) Multifunctional self-assembling hydrogel from guar gum. Chem Eng J 330:1044–1051. https://doi.org/10.1016/j.cej.2017.08.041

Duan C, Zhao N, Yu X et al (2013) Chemically modified kapok fiber for fast adsorption of Pb^{2+}, Cd^{2+}, Cu^{2+} from aqueous solution. Cellulose 20:849–860. https://doi.org/10.1007/s10570-013-9875-9

Erdtman H (1972) Lignins: occurrence, formation, structure and reactions, K. V. Sarkanen and C. H. Ludwig, Eds., John Wiley & Sons, Inc., New York, 1971. 916pp. $35.00. J Polym Sci [B] 10:228–230. https://doi.org/10.1002/pol.1972.110100315

Fujisawa S, Togawa E, Hayashi N (2016) Orientation control of cellulose nanofibrils in all-cellulose composites and

mechanical properties of the films. J Wood Sci 62:174–180. https://doi.org/10.1007/s10086-015-1533-4

Gautam RK, Mudhoo A, Lofrano G, Chattopadhyaya MC (2014) Biomass-derived biosorbents for metal ions sequestration: adsorbent modification and activation methods and adsorbent regeneration. J Environ Chem Eng 2:239–259. https://doi.org/10.1016/j.jece.2013.12.019

Ge Y, Xiao D, Li Z, Cui X (2014) Dithiocarbamate functionalized lignin for efficient removal of metallic ions and the usage of the metal-loaded bio-sorbents as potential free radical scavengers. J Mater Chem A 2:2136–2145. https://doi.org/10.1039/C3TA14333C

Gidh AV, Decker SR, Vinzant TB et al (2006) Determination of lignin by size exclusion chromatography using multi angle laser light scattering. J Chromatogr A 1114:102–110. https://doi.org/10.1016/j.chroma.2006.02.044

Guerra A, Gaspar AR, Contreras S et al (2007) On the propensity of lignin to associate: a size exclusion chromatography study with lignin derivatives isolated from different plant species. Phytochemistry 68:2570–2583. https://doi.org/10.1016/j.phytochem.2007.05.026

Guo X, Zhang S, Shan X (2008) Adsorption of metal ions on lignin. J Hazard Mater 151:134–142. https://doi.org/10.1016/j.jhazmat.2007.05.065

Hajeeth T, Vijayalakshmi K, Gomathi T, Sudha PN (2013) Removal of Cu(II) and Ni(II) using cellulose extracted from sisal fiber and cellulose-g-acrylic acid copolymer. Int J Biol Macromol 62:59–65. https://doi.org/10.1016/j.ijbiomac.2013.08.029

Ho Y (2006) Review of second-order models for adsorption systems. J Hazard Mater 136:681–689. https://doi.org/10.1016/j.jhazmat.2005.12.043

Hokkanen S, Repo E, Suopajärvi T et al (2014) Adsorption of Ni(II), Cu(II) and Cd(II) from aqueous solutions by amino modified nanostructured microfibrillated cellulose. Cellulose 21:1471–1487. https://doi.org/10.1007/s10570-014-0240-4

Isobe N, Chen X, Kim U-J et al (2013) TEMPO-oxidized cellulose hydrogel as a high-capacity and reusable heavy metal ion adsorbent. J Hazard Mater 260:195–201. https://doi.org/10.1016/j.jhazmat.2013.05.024

Isogai A, Saito T, Fukuzumi H (2011) TEMPO-oxidized cellulose nanofibers. Nanoscale 3:71–85. https://doi.org/10.1039/C0NR00583E

Jung KA, Woo SH, Lim S-R, Park JM (2015) Pyrolytic production of phenolic compounds from the lignin residues of bioethanol processes. Chem Eng J 259:107–116. https://doi.org/10.1016/j.cej.2014.07.126

Kamel S, Hassan EM, El-Sakhawy M (2006) Preparation and application of acrylonitrile-grafted cyanoethyl cellulose for the removal of copper (II) ions. J Appl Polym Sci 100:329–334. https://doi.org/10.1002/app.23317

Kumar PS, Ramalingam S, Kirupha SD et al (2011) Adsorption behavior of nickel(II) onto cashew nut shell: equilibrium, thermodynamics, kinetics, mechanism and process design. Chem Eng J 167:122–131. https://doi.org/10.1016/j.cej.2010.12.010

Li Z, Kong Y, Ge Y (2015a) Synthesis of porous lignin xanthate resin for Pb^{2+} removal from aqueous solution. Chem Eng J 270:229–234. https://doi.org/10.1016/j.cej.2015.01.123

Li Z, Xiao D, Ge Y, Koehler S (2015b) Surface-functionalized porous lignin for fast and efficient lead removal from aqueous solution. ACS Appl Mater Interfaces 7:15000–15009. https://doi.org/10.1021/acsami.5b03994

Lindströmn T (1979) The colloidal behaviour of kraft lignin. Colloid Polym Sci 257:277–285. https://doi.org/10.1007/BF01382370

Liu L, Wang R, Yu J et al (2016) Robust self-standing chitin nanofiber/nanowhisker hydrogels with designed surface charges and ultralow mass content via gas phase coagulation. Biomacromolecules 17:3773–3781. https://doi.org/10.1021/acs.biomac.6b01278

Liu Y, Deng L, Zhang C et al (2018) Tunable physical properties of ethylcellulose/gelatin composite nanofibers by electrospinning. J Agric Food Chem 66:1907–1915. https://doi.org/10.1021/acs.jafc.7b06038

Ma J, Zhou G, Chu L et al (2017) Efficient removal of heavy metal ions with an EDTA functionalized chitosan/polyacrylamide double network hydrogel. ACS Sustain Chem Eng 5:843–851. https://doi.org/10.1021/acssuschemeng.6b02181

Ma J, Liu Y, Ali O et al (2018) Fast adsorption of heavy metal ions by waste cotton fabrics based double network hydrogel and influencing factors insight. J Hazard Mater 344:1034–1042. https://doi.org/10.1016/j.jhazmat.2017.11.041

Mahfoudhi N, Boufi S (2017) Nanocellulose as a novel nanostructured adsorbent for environmental remediation: a review. Cellulose 24:1171–1197. https://doi.org/10.1007/s10570-017-1194-0

Minu K, Jiby KK, Kishore VVN (2012) Isolation and purification of lignin and silica from the black liquor generated during the production of bioethanol from rice straw. Biomass Bioenergy 39:210–217. https://doi.org/10.1016/j.biombioe.2012.01.007

Mohammadi Z, Shangbin S, Berkland C, Liang J (2017) Chelator-mimetic multi-functionalized hydrogel: highly efficient and reusable sorbent for Cd, Pb, and As removal from waste water. Chem Eng J 307:496–502. https://doi.org/10.1016/j.cej.2016.08.121

Mohan D, Pittman CU, Steele PH (2006) Single, binary and multi-component adsorption of copper and cadmium from aqueous solutions on Kraft lignin—a biosorbent. J Colloid Interface Sci 297:489–504. https://doi.org/10.1016/j.jcis.2005.11.023

Mushi NE, Kochumalayil J, Cervin NT et al (2016) Nanostructurally controlled hydrogel based on small-diameter native chitin nanofibers: preparation, structure, and properties. ChemSusChem 9:989–995. https://doi.org/10.1002/cssc.201501697

Pagnanelli F, Mainelli S, Vegliò F, Toro L (2003) Heavy metal removal by olive pomace: biosorbent characterisation and equilibrium modelling. Chem Eng Sci 58:4709–4717. https://doi.org/10.1016/j.ces.2003.08.001

Pang Y, Wang S, Qiu X et al (2017) Preparation of lignin/sodium dodecyl sulfate composite nanoparticles and their application in pickering emulsion template-based microencapsulation. J Agric Food Chem 65:11011–11019. https://doi.org/10.1021/acs.jafc.7b03784

Qi H, Cai J, Zhang L, Kuga S (2009) Properties of films composed of cellulose nanowhiskers and a cellulose matrix

regenerated from alkali/urea solution. Biomacromolecules 10:1597–1602. https://doi.org/10.1021/bm9001975

Qian S, Sheng K (2017) PLA toughened by bamboo cellulose nanowhiskers: role of silane compatibilization on the PLA bionanocomposite properties. Compos Sci Technol 148:59–69. https://doi.org/10.1016/j.compscitech.2017.05.020

Safwat E, Hassan ML, Saniour S et al (2018) Injectable TEMPO-oxidized nanofibrillated cellulose/biphasic calcium phosphate hydrogel for bone regeneration. J Biomater Appl. https://doi.org/10.1177/0885328218763866

Sehaqui H, de Larraya UP, Liu P et al (2014) Enhancing adsorption of heavy metal ions onto biobased nanofibers from waste pulp residues for application in wastewater treatment. Cellulose 21:2831–2844. https://doi.org/10.1007/s10570-014-0310-7

Shi Z, Yang Q, Kuga S, Matsumoto Y (2015) Dissolution of wood pulp in aqueous NaOH/urea solution via dilute acid pretreatment. J Agric Food Chem 63:6113–6119. https://doi.org/10.1021/acs.jafc.5b01714

Simonin J-P (2016) On the comparison of pseudo-first order and pseudo-second order rate laws in the modeling of adsorption kinetics. Chem Eng J 300:254–263. https://doi.org/10.1016/j.cej.2016.04.079

Sotto A, Kim J, Arsuaga JM et al (2014) Binary metal oxides for composite ultrafiltration membranes. J Mater Chem A 2:7054–7064. https://doi.org/10.1039/C3TA15347A

Srivastava SK, Singh AK, Sharma A (1994) Studies on the uptake of lead and zinc by lignin obtained from black liquor—a paper industry waste material. Environ Technol 15:353–361. https://doi.org/10.1080/09593339409385438

Suhas Gupta VK, Carrott PJM et al (2016) Cellulose: a review as natural, modified and activated carbon adsorbent. Bioresour Technol 216:1066–1076. https://doi.org/10.1016/j.biortech.2016.05.106

Wang Z, Liu S, Matsumoto Y, Kuga S (2012) Cellulose gel and aerogel from LiCl/DMSO solution. Cellulose 19:393–399. https://doi.org/10.1007/s10570-012-9651-2

Wang Q, Shi X, Xu J et al (2016) Highly enhanced photocatalytic reduction of Cr(VI) on AgI/TiO2 under visible light irradiation: influence of calcination temperature. J Hazard Mater 307:213–220. https://doi.org/10.1016/j.jhazmat.2015.12.050

Wang Z, Yu J, Zhang L et al (2017) Cellulose laurate ester aerogel as a novel absorbing material for removing pollutants from organic wastewater. Cellulose 24:5069–5078. https://doi.org/10.1007/s10570-017-1489-1

Weber WJ, Morris JC (1963) Kinetics of adsorption on carbon from solution. J Sanit Eng Div 89:31–60

Xiong J, Jiao C, Li C et al (2014) A versatile amphiprotic cotton fiber for the removal of dyes and metal ions. Cellulose 21:3073–3087. https://doi.org/10.1007/s10570-014-0318-z

Xu Y, Li K, Zhang M (2007) Lignin precipitation on the pulp fibers in the ethanol-based organosolv pulping. Colloids Surf Physicochem Eng Asp 301:255–263. https://doi.org/10.1016/j.colsurfa.2006.12.078

Xu X, Liu F, Jiang L et al (2013) Cellulose nanocrystals vs. cellulose nanofibrils: a comparative study on their microstructures and effects as polymer reinforcing agents. ACS Appl Mater Interfaces 5:2999–3009. https://doi.org/10.1021/am302624t

Xu Z, Gao G, Pan B et al (2015) A new combined process for efficient removal of Cu(II) organic complexes from wastewater: Fe(III) displacement/UV degradation/alkaline precipitation. Water Res 87:378–384. https://doi.org/10.1016/j.watres.2015.09.025

Zeng L, Chen Y, Zhang Q et al (2015) Adsorption of Cd(II), Cu(II) and Ni(II) ions by cross-linking chitosan/rectorite nano-hybrid composite microspheres. Carbohydr Polym 130:333–343. https://doi.org/10.1016/j.carbpol.2015.05.015

Zhang L, Yan L, Wang Z et al (2015) Characterization of lignin derived from water-only and dilute acid flowthrough pretreatment of poplar wood at elevated temperatures. Biotechnol Biofuels 8:203. https://doi.org/10.1186/s13068-015-0377-x

Zhang N, Zang G-L, Shi C et al (2016) A novel adsorbent TEMPO-mediated oxidized cellulose nanofibrils modified with PEI: preparation, characterization, and application for Cu(II) removal. J Hazard Mater 316:11–18. https://doi.org/10.1016/j.jhazmat.2016.05.018

Zhang L, Lu H, Yu J et al (2017) Dissolution of lignocelluloses with a high lignin content in a N-methylmorpholine-N-oxide monohydrate solvent system via simple glycerol-swelling and mechanical pretreatments. J Agric Food Chem 65:9587–9594. https://doi.org/10.1021/acs.jafc.7b03429

Zhao W, Yang L, He L, Zhang S (2016) Simultaneous enrichment of polycyclic aromatic hydrocarbons and Cu^{2+} in water using tetraazacalix[2]arene[2]triazine as a solid-phase extraction selector. J Agric Food Chem 64:6233–6239. https://doi.org/10.1021/acs.jafc.6b03083

Zhu Q, Li Z (2015) Hydrogel-supported nanosized hydrous manganese dioxide: synthesis, characterization, and adsorption behavior study for Pb^{2+}, Cu^{2+}, Cd^{2+} and Ni^{2+} removal from water. Chem Eng J 281:69–80. https://doi.org/10.1016/j.cej.2015.06.068